

Presented at Sixth University
Conference on Ceramic Science,
North Carolina State University,
December 7-9, 1970

UCRL-20383
Preprint

MASTER

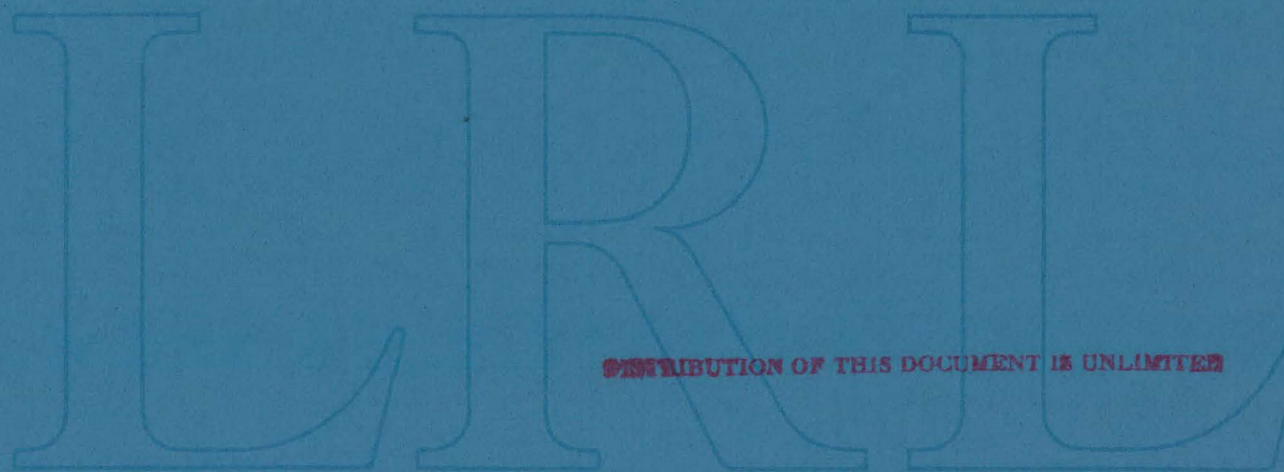
CONF-701206--2

FACTORS INFLUENCING THE STRESS-STRAIN
BEHAVIOR OF CERAMIC MATERIALS

Terence G. Langdon and Joseph A. Pask

December 1970

AEC Contract No. W-7405-eng-48



DISTRIBUTION OF THIS DOCUMENT IS UNLIMITED

LAWRENCE RADIATION LABORATORY
UNIVERSITY of CALIFORNIA BERKELEY

UCRL-20383

DISCLAIMER

This report was prepared as an account of work sponsored by an agency of the United States Government. Neither the United States Government nor any agency Thereof, nor any of their employees, makes any warranty, express or implied, or assumes any legal liability or responsibility for the accuracy, completeness, or usefulness of any information, apparatus, product, or process disclosed, or represents that its use would not infringe privately owned rights. Reference herein to any specific commercial product, process, or service by trade name, trademark, manufacturer, or otherwise does not necessarily constitute or imply its endorsement, recommendation, or favoring by the United States Government or any agency thereof. The views and opinions of authors expressed herein do not necessarily state or reflect those of the United States Government or any agency thereof.

DISCLAIMER

Portions of this document may be illegible in electronic image products. Images are produced from the best available original document.

LEGAL NOTICE

This report was prepared as an account of work sponsored by the United States Government. Neither the United States nor the United States Atomic Energy Commission, nor any of their employees, nor any of their contractors, subcontractors, or their employees, makes any warranty, express or implied, or assumes any legal liability or responsibility for the accuracy, completeness or usefulness of any information, apparatus, product or process disclosed, or represents that its use would not infringe privately owned rights.

-1-

UCRL-20383

FACTORS INFLUENCING THE STRESS-STRAIN
BEHAVIOR OF CERAMIC MATERIALS

Terence G. Langdon* and Joseph A. Pask

Inorganic Materials Research Division, Lawrence Radiation Laboratory,
and Department of Materials Science and Engineering,
College of Engineering, University of California,
Berkeley, California

INTRODUCTION

Although ceramic materials are of considerable potential interest, because of their ability to withstand high temperatures and severe corrosion environments, their use has so far been limited by brittleness and poor resistance to thermal shock. A large volume of work over the last decade has shown that several factors influence the stress-strain behavior observed in ceramic systems, ranging from the presence of point defects in single crystals to the size and location of pores in polycrystals. Furthermore, the complexity of this influence may be illustrated by noting that the behavior of nominally identical single crystals is markedly dependent on whether impurities are present as isolated point defects, as aggregates, or in the form of pairs of impurity atoms and charge-compensating vacancies.

This paper reviews the primary factors influencing the stress-strain behavior of single crystals, and discusses some recent results obtained on polycrystalline magnesium oxide. For simplicity, emphasis is placed on systems having the rock salt structure, and the effect of changes in stoichiometry, important in materials such as UO_2 and ThO_2 , is not included.

*Now at University of British Columbia.

FACTORS INFLUENCING THE BEHAVIOR OF SINGLE CRYSTALS

Under a constant rate of strain or loading, a single crystal tested in tension or compression deforms elastically up to the critical resolved shear stress (CRSS) at which plastic flow begins.

An analysis of the temperature dependence of the CRSS (or the yield stress) is most conveniently carried out by considering the schematic curves in Fig. 1, in which the behavior for a given strain rate, $\dot{\epsilon}_1$, is divided into three distinct regions. At low temperatures (region I), typically $\lesssim 0.2-0.3 T_m$ where T_m is the absolute melting temperature, the CRSS decreases rapidly with increasing temperature, and the behavior is controlled by thermal fluctuations which permit the dislocations to overcome short-range obstacles in the glide plane (e.g. solute atoms or the Peierls barrier). In region II, the CRSS drops only slightly with increasing temperature, and the controlling mechanism is then athermal (e.g. overcoming of long-range stress fields); the slight temperature dependence in this region arises from the decrease in shear modulus with increasing temperature. At high temperatures (region III), typically $\lesssim 0.5 T_m$, diffusion plays a significant role, and the CRSS again drops. It should also be noted that these three regions are not delineated by fixed temperature boundaries; a faster strain rate, such as $\dot{\epsilon}_2 (> \dot{\epsilon}_1)$, moves the transitions to higher temperatures. Finally, region IV corresponds to very rapid strain rates ($\dot{\epsilon}_3 \gg \dot{\epsilon}_2$), as in impact tests, where the motion of dislocations is limited by viscous damping.

Factors influencing the behavior in regions I and II are now examined; the deformation mechanisms of importance in region III, which corresponds essentially to the "high-temperature creep" range, are not considered here, but are dealt with in detail in the following paper.¹

Effect of Surface Condition

The surface condition of ionic crystals is important in determining the shape of the stress-strain curve; a detailed review of the extensive work on magnesium oxide is given elsewhere.² Stokes³ showed that MgO crystals containing "fresh" dislocation sources, due to cleavage or mechanical contact, yielded smoothly in tension at $\sim 6-8000$ psi. However, if the "fresh" sources were eliminated by chemical polishing, the crystals deformed elastically up to stresses of $\sim 30-50,000$ psi before yielding with a sharp drop in stress down to the level at which the "fresh" dislocations moved. These experiments emphasize the significance of the surface condition, and serve to show that the "grown in" dislocations in MgO are immobile.

Effect of Strain Rate

As indicated in Fig. 1, an increase in strain rate at any given temperature results in a higher CRSS in the thermally-activated region I, but there is no change in region II. An experimental example is shown in Fig. 2 for NaCl crystals having a $\langle 100 \rangle$ axis tested at two different strain rates,⁴ where the CRSS, τ_c , is divided by the shear modulus, G , so that the results in region II are independent of temperature. At temperatures less than $\sim 250^\circ\text{K}$, the experimental points for the two strain rates are different, and, within the error bars indicated, the results are reasonably approximated by the two straight lines converging to $\tau_c/G \sim 7.8 \times 10^{-5}$ at $T = 0^\circ\text{K}$.

Although Fig. 2 refers to only a modest increase in $\dot{\epsilon}$, tests have also been carried out on MgO crystals at very rapid strain rates.⁵ Results are given in Fig. 3 for values of $\dot{\epsilon}$ ranging from 10^{-4} sec⁻¹

(which is comparable to the usual stress-strain data) to $3 \times 10^3 \text{ sec}^{-1}$, thereby showing the transition to region IV indicated in Fig. 1.

Effect of Orientation

The orientation of a crystal determines the magnitude of the resolved shear stress acting on the slip planes. For crystals of the rock salt structure, slip takes place preferentially on the $\{110\} \langle 1\bar{1}0 \rangle$ slip systems, although flow is also possible on the $\{001\} \langle 1\bar{1}0 \rangle$ systems at higher temperatures or stresses. For a crystal tested in compression with a $\langle 100 \rangle$ longitudinal axis, which represents the usual cleaved condition, there is a resolved shear stress equal to one half of the applied stress acting on four of the six $\{110\} \langle 1\bar{1}0 \rangle$ slip systems; the other two systems experience no stress. For a $\langle 111 \rangle$ loading axis, however, there is no resolved shear stress acting on any of the $\{110\} \langle 1\bar{1}0 \rangle$ slip systems, so that crystals then deform at the higher temperatures by slip on the $\{001\} \langle 1\bar{1}0 \rangle$ slip systems; at low temperatures the crystals fracture without any plastic deformation. The importance of this orientation difference is illustrated in Fig. 4 for MgO crystals tested at a constant rate of loading of 20 psi/sec;^{6,7,8} for the $\langle 100 \rangle$ axis there is only a slight decrease for temperatures above $\sim 1000^\circ\text{C}$, but the values obtained for crystals with a $\langle 111 \rangle$ axis are substantially higher and are still decreasing sharply even at the highest indicated test temperature.

Effect of Impurity Concentration

Impurities play a major role in determining stress-strain behavior, even when the concentration is relatively small. For example, Gorum et al.⁹ showed that the yield stress for an MgO crystal containing 30 ppm of iron was about four times higher than for a crystal containing only

10 ppm. By contrast, a further increase in iron content to 3000 ppm increased the yield stress only slightly.

The CRSS in alkali halide crystals is extremely sensitive to the presence of divalent cations. Using NaCl crystals, Hesse¹⁰ showed that an increase in Ca^{2+} concentration from 2 to 20 ppm increased the athermal plateau (region II) and, because of the larger number of obstacles, introduced a greater temperature-sensitivity in the thermally-activated region I. There is also a marked difference in the shape of the stress-strain curves for different impurity concentrations, as shown in Fig. 5 for NaCl crystals tested at 294°K with Ca^{2+} concentrations of 2, 33 and 64 ppm, respectively.¹¹ In particular, the slope and length of stage I increases with increasing impurity content.

Effect of Nature of Impurities

Whilst small variations in the concentration of impurities significantly affect the stress-strain behavior, the magnitude of this influence is dependent on both the state of dispersion and the valency of the impurities in question. This is illustrated in Fig. 6. For "pure" LiF crystals, containing 3 ppm Mg^{2+} , the CRSS increases only slightly at very low temperatures, and there is no significant difference between crystals slowly cooled ($\sim 0.002^\circ\text{C}/\text{min}$; solid line) and air-cooled ($\sim 50^\circ\text{C}/\text{min}$; dashed line) from an annealing treatment at 300°C. By contrast, the behavior of "impure" crystals, containing 75 ppm Mg^{2+} , depends critically on thermal history: for air-cooled crystals, the athermal stress level (region II) is only slightly higher than for the "pure" crystals, but there is a pronounced increase in CRSS in the thermally-activated region I; for slowly cooled crystals, the CRSS in region II is very much

increased, but the temperature dependence in region I is less pronounced.¹² This suggests that in the slowly cooled crystals the impurities are primarily present in clusters or precipitates. A further complexity may also arise since, whereas these results for Mg^{2+} in LiF show a quench softening, so that the CRSS at room temperature is less for air-cooled crystals than for slow-cooled, NaCl crystals doped with large concentrations of Mn^{2+} and Cd^{2+} show a quench hardening.¹³

In magnesium oxide, the presence of Fe^{3+} leads to considerable hardening, but Ni^{2+} in the absence of iron has only a small effect. This is shown in Fig. 7, using room temperature data reported by Srinivasan and Stoebe¹⁴ and Moon and Pratt¹⁵ (note that the point for 130 ppm Fe^{3+} was obtained by extrapolation of the published data¹⁵). This plot suggests that, over the limited range examined, τ_c is approximately linearly proportional to c , where c is the defect concentration, but results by Davidge¹⁶ indicate τ_c is proportional to $c^{1/2}$ over a range of 100-1400 ppm of Fe^{3+} . The differing hardening effects of Ni^{2+} and Fe^{3+} in MgO are thus analogous to the effects of mono- and divalent impurities in the alkali halides (compare, for example, Fig. 6 with Fig. 23 of the review by Gilman¹⁷). The significance of valency is also shown by noting that the CRSS for MgO crystals heat treated in air to give 6 ± 1 ppm of iron in the Fe^{3+} state was 1.1 ± 0.07 kg/mm² (1560 ± 100 psi), whereas identical crystals given a reducing treatment at 2000°C, so that the iron was present as Fe^{2+} , gave a CRSS of only 0.73 ± 0.07 kg/mm² (1040 ± 100 psi).¹⁴

It may be initially anticipated that plastic flow in ionic crystals at the low temperatures is governed by a form of Peierls mechanism,

because of the necessity for the dislocations to overcome Coulombic interactions. However, the experimental data presented in Fig. 6 show that the behavior is dependent on the presence of impurities. To explain the large temperature-sensitivity of the air-cooled "impure" LiF crystals, a theory was developed in which the hardening was attributed to the tetragonal lattice distortions produced by an impurity (Mg^{2+})-vacancy dipole.¹⁸ This theory predicts a linear relationship between $\tau^*{}^{1/2}$ and $T^{1/2}$, where τ^* is the effective stress (equal to the measured CRSS minus the athermal stress, τ_A ; see Fig. 1) and T is the absolute temperature, in agreement with the data shown in Fig. 8. The theory also predicts a linearity between τ^* and $c^{1/2}$; this agrees with experiments at low temperatures but some results at higher temperatures (e.g. in NaCl at room temperature for Ca^{2+} concentrations of up to 900 mole ppm¹³) show τ^* is linearly proportional to c . These latter results have been interpreted by assuming that the impurity-vacancy dipoles are then able to rotate in the strain field of the dislocations, thereby lowering the elastic energy of the system.¹⁹

The situation for MgO is somewhat different since, although one cation vacancy is required for charge compensation for every two Fe^{3+} ions incorporated in the lattice, electron spin resonance indicates that these are not contained in the form of ion-vacancy pairs¹⁶; in this case the hardening may arise because the excess vacancies, or the presence of Fe^{3+} ions on interstitial sites, increase the rate of jog formation on the screw dislocations.

Effect of Pressure

Experiments show that the CRSS is independent of pressure for NaCl crystals of $\langle 100 \rangle$ orientation up to 10 kbars²⁰ and MgO crystals of $\langle 111 \rangle$

orientation up to 5 kbars,²¹ respectively. But it should be noted that the situation is more complex for polycrystalline materials, and in MgO there is a brittle-ductile transition with increasing pressure, so that large strains ($\geq 10\%$) may be achieved at room temperature without fracture.²¹

Effect of Irradiation

Irradiation produces a hardening in alkali halides, the magnitude of which depends on the time, temperature, intensity, and nature of the radiation, and the impurity level of the crystal. The theory of asymmetrical defects¹⁸ has been used to interpret the magnitude and temperature dependence of radiation hardening in Ag-doped KCl;²² but the theory predicts that defect alignment will lead to anisotropic hardening, and this is not observed experimentally.²³

FACTORS INFLUENCING THE BEHAVIOR OF POLYCRYSTALS

Whilst the preceding section shows that several factors significantly influence the stress-strain behavior of single crystals, the situation for polycrystalline materials is more complex. In particular, four additional features should be considered.

Firstly, impurities may further influence the deformation behavior in polycrystals due to preferential segregation at the grain boundaries, either as a second phase or in solid solution. For example, it has been shown that some common impurities in polycrystalline MgO, such as Al, Ca and Si, segregate to the boundaries even when only present in amounts as small as 30 atomic ppm, although other impurities, such as Fe, tend to be more uniformly distributed.²⁴ More complex ceramic systems may have a silicate phase at the boundary.

Secondly, the density of polycrystalline ceramics is invariably less than the theoretical value for single crystals. As discussed in the following section, the influence of this residual porosity depends on such features as the primary pore location (i.e. whether along the grain boundaries or within the grains), the size and distribution of the intragranular pores, and the average size of the boundary pores with respect to the grain size.

Thirdly, a polycrystalline material is only capable of deforming plastically, without the nucleation of internal voids, when it possesses five independent slip systems. This requirement is fulfilled in the rock salt structure when slip occurs on both the $\{110\} \langle 1\bar{1}0 \rangle$ and $\{001\} \langle 1\bar{1}0 \rangle$ slip systems; in MgO, this necessitates either high temperatures or the ability for large stress concentrations to build up at the boundaries and thereby nucleate slip on the $\{100\}$ planes.

Fourthly, it is necessary that these various slip systems are capable of interpenetration. A detailed investigation of MgO single crystals, tested in tension at an initial strain rate of $\sim 6.7 \times 10^{-4} \text{ sec}^{-1}$, showed that the 90° intersections due to slip on conjugate planes, which form neutral (i.e. uncharged) jogs, are only possible at temperatures of 1300°C and above, and the 60° and 120° intersections due to slip on oblique planes, which form electrostatically charged jogs, only occur above 1700°C ;²⁵ although these temperatures may be lowered by a reduction in strain rate. In conformity with these results, tensile tests on recrystallized polycrystalline MgO show a brittle-ductile transition at $\sim 1700^\circ\text{C}$.²⁶ In compression tests, however, catastrophic failure is more difficult, and large stresses can then build up to aid the nucleation

and interpenetration of the different slip systems at lower temperatures; for example, the 90° intersections become possible at temperatures as low as 1200°C .

Stress-Strain Behavior of Polycrystalline MgO

The considerable significance of small changes in microstructural detail is demonstrated by results obtained from compression tests on six different types of polycrystalline MgO.²⁷ All of these materials deformed plastically at 1200°C and above, but two types (5 and 6) exhibited plastic flow at temperatures as low as 800°C and a third (type 4) at 1000°C .

Examples of the microstructures of types 1-4 are shown in Fig. 9. Type 1 (lower left) was produced by hot pressing MgO powder with a 3 wt % LiF additive, giving a transparent material which was nominally fully-dense but with a residual Li content of 75 ppm. Although electron microscopy showed that no second phase existed at the grain boundaries,²⁸ the occurrence of much intergranular fracture at low temperatures in comparison with specimens without an additive suggested that LiF was probably preferentially segregated at the boundaries in solid solution. Type 2 (lower right), 3 (upper left) and 4 (upper right) were produced by isostatic pressing and sintering, and were typically $\sim 1.5\%$ porous but with variations in the average pore size and distribution. The microstructure of type 5, which was one of the two materials deforming plastically at the lower temperatures, is shown in greater detail in Fig. 10. This material was also $\sim 1.5\%$ porous, and was obtained by annealing the type 6 material at 1800°C . The pore-free regions adjacent to many of the grain boundaries probably represent the areas swept out

during grain growth from the initial average grain size of 25 μm to the final size of 80 μm .

Although the microstructures of these materials appear fairly similar, the stress-strain curves reveal significant differences; this may be seen by comparing the results at 800°C and 1000°C, as shown in Figs. 11 and 12, respectively. At 800°C, types 1-4 were not ductile, but types 5 and 6 deformed to strains >0.02 . Type 1 fractured at $\sim 40,000$ psi, represented by the vertical arrow, but the tests on types 2-4 were discontinued prior to fracture at $\sim 45,000$ psi. At 1000°C, types 1-3 fractured with little significant plastic deformation at stresses in the range $\sim 29-45,000$ psi, but types 4-6 deformed to strains >0.02 . All specimens were ductile to strains in excess of 0.02 at 1200°C.

Figure 13 shows the yield stresses calculated from a strain offset of 5×10^{-4} as a function of temperature, together with the data described earlier for single crystals having $\langle 100 \rangle$ and $\langle 111 \rangle$ loading axes; the closed symbol for type 1 at 1000°C represents a fracture stress when no yielding occurred. The values recorded for types 5 and 6 are lower than for the $\langle 111 \rangle$ loaded single crystals, and this at first suggests that no slip occurred on the $\{001\} \langle 1\bar{1}0 \rangle$ slip systems. However, wavy slip lines resulting from slip on both the $\{110\}$ and $\{100\}$ systems were visible on the surfaces of these specimens after testing at temperatures as low as 800°C, although no wavy slip was observed in types 1-3 at temperatures below 1200°C. This indicates that stress levels of sufficient magnitude were able to build up at the grain boundaries in types 5 and 6 to realize flow on the secondary slip systems.

The marked differences in behavior for materials of similar density ($\sim 8.5\%$) show that the microstructural features influencing the stress-strain relations in polycrystals are fairly complex, particularly since the realization of general ductility at 1200°C corresponds with the temperature at which such behavior is obtained for single crystals with $\langle 100 \rangle$ and $\langle 111 \rangle$ orientations,^{7,8} as indicated for the latter orientation in Fig. 14. An analysis of the experimental observations in terms of the material characteristics of the various specimen types, described in detail elsewhere,²⁷ suggests two factors which aid plasticity at temperatures below $\sim 1200^\circ\text{C}$:

(i) The grain boundaries should be sufficiently strong to allow the build-up of stress concentrations and nucleation of slip on the $\{100\}$ system and to permit extension of slip bands across the boundaries. This requires (a) that they are relatively pore-free, and if boundary pores exist they should be small with respect to the grain size, and (b) that they are free from excessive amounts of impurities in solid solution. Condition (a) is not fulfilled in type 2, where the ratio of boundary pores to grain size is ~ 0.2 ; condition (b) is not fulfilled in type 1 due to the residual LiF which appears to weaken the grain boundaries, or in type 3 due to a higher amount of SiO_2 and CaO content which appear to interfere with dislocation motion.

(ii) Very fine pores distributed within the grains appear to be beneficial, probably because they permit some mass accommodation required because of the limited slip activity. Types 5 and 6 are examples of fairly pure materials containing fine intragranular porosity.

SUMMARY AND CONCLUSIONS

The factors influencing the stress-strain behavior of single crystals are briefly reviewed. It is shown that the results obtained under a given set of experimental conditions depend on features ranging from crystal orientation, which is readily determined, to less controllable parameters such as the presence, and in particular the state of dispersion, of certain impurities. Further complexities arise in polycrystals because of impurity segregation at the boundaries, the presence and nature of residual porosity, and problems associated with the availability, and interpenetration, of the various slip systems.

An examination of experimental results obtained on several different types of polycrystalline MgO suggests that ductility is aided at temperatures less than $\sim 1200^{\circ}\text{C}$ by the presence of strong grain boundaries and by very fine intragranular porosity.

ACKNOWLEDGMENT

This work was done under the auspices of the United States Atomic Energy Commission.

REFERENCES

1. T. G. Langdon, D. R. Cropper and J. A. Pask, "Creep Mechanisms in Ceramic Materials at Elevated Temperatures," Materials Science Research, Volume 6, (this volume).
2. T. G. Langdon and J. A. Pask, "Mechanical Behavior of Single-Crystal and Polycrystalline MgO;" pp. 53-127 in High Temperature Oxides - Volume III. Edited by A. Alper. Academic Press, New York, 1970.
3. R. J. Stokes, "Dislocation Sources and the Strength of Magnesium Oxide Single Crystals," Trans. AIME, 224 (12) 1227-37 (1962).
4. J. Hesse, "Die plastische Verformung von Natriumchlorid," Phys. Stat. Sol., 9 (1), 209-30 (1965).
5. A. Kumar, "Strain Rate Effects in Materials;" pp. 67-96 in High Speed Testing - Volume VII. Interscience, New York, 1969.
6. C. O. Hulse and J. A. Pask, "Mechanical Properties of Magnesia Single Crystals in Compression," J. Amer. Ceram. Soc., 43 (7) 373-78 (1960).
7. C. O. Hulse, S. M. Copley and J. A. Pask, "Effect of Crystal Orientation on Plastic Deformation of Magnesium Oxide," J. Am. Ceram. Soc., 46 (7) 317-23 (1963).
8. S. M. Copley and J. A. Pask, "Plastic Deformation of MgO Single Crystals up to 1600°C," J. Am. Ceram. Soc., 48 (3) 139-46 (1965).
9. A. E. Gorum, W. J. Luhman and J. A. Pask, "Effect of Impurities and Heat-Treatment on Ductility of MgO," J. Am. Ceram. Soc., 43 (5) 241-45 (1960).
10. J. Hesse, "Zur Verfestigung Reiner und Schwach Dotierter NaCl-Kristalle;" pp. 413-20 in Reinststoffprobleme - Volume III. Edited

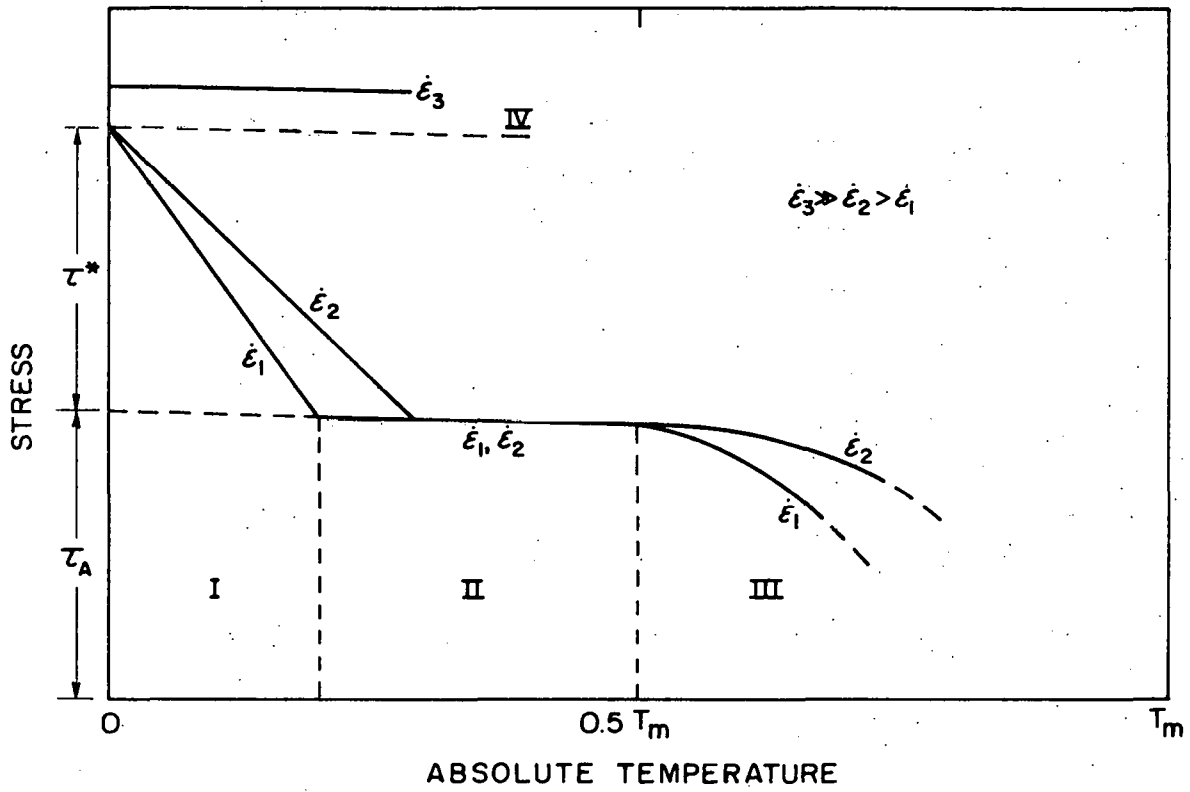
- by E. Rexer. Akademie-Verlag, Berlin, 1967.
11. J. Hesse, "Fließspannung und Versetzungsdichte Kalzium-dotierter NaCl-Einkristalle," *Phys. Stat. Sol.*, 21 (2) 495-505 (1967).
 12. W. G. Johnston, "Effect of Impurities on the Flow Stress of LiF Crystals," *J. Appl. Phys.*, 33 (6) 2050-58 (1962).
 13. P. L. Pratt, R. P. Harrison and C. W. A. Newey, "Dislocation Mobility in Ionic Crystals," *Discs. Faraday Soc.*, 38 211-17 (1964).
 14. M. Srinivasan and T. G. Stoebe, "Effect of Impurities on the Mechanical Behavior of MgO Single Crystals," *J. Appl. Phys.*, 41 (9) 3726-30 (1970).
 15. R. L. Moon and P. L. Pratt, "Compression of MgO Single Crystals Containing Low Concentrations of Iron," *Proc. Brit. Ceram. Soc.*, 15 203-14 (1970).
 16. R. W. Davidge, "The Distribution of Iron Impurity in Single-Crystal Magnesium Oxide and Some Effects on Mechanical Properties," *J. Mater. Sci.*, 2 (4) 339-46 (1967).
 17. J. J. Gilman, "Mechanical Behavior of Ionic Crystals," *Progress in Ceramic Science*, 1 146-99 (1961).
 18. R. L. Fleischer, "Rapid Solution Hardening, Dislocation Mobility, and the Flow Stress of Crystals," *J. Appl. Phys.*, 33 (12) 3504-08 (1962).
 19. P. L. Pratt, R. Chang and C. W. A. Newey, "Effect of Divalent Metal Impurity Distribution, Quenching Rate, and Annealing Temperature on Flow Stress in Ionic Crystals," *Appl. Phys. Letters*, 3 (5) 83-85 (1963).

20. E. Aladag, L. A. Davis and R. B. Gordon, "Cross Slip and the Plastic Deformation of NaCl Single and Polycrystals at High Pressure," *Phil. Mag.*, 21 (171) 469-78 (1970).
21. M. S. Paterson and C. W. Weaver, "Deformation of Polycrystalline MgO Under Pressure," *J. Am. Ceram. Soc.*, 53 (8) 463-71 (1970).
22. J. S. Nadeau, "Hardening of Silver-Doped Potassium Chloride by Low-Temperature X-Ray Irradiation," *J. Appl. Phys.*, 37 (4) 1602-08 (1966).
23. J. S. Nadeau, "The Mechanical Properties of Irradiated Alkali Halide Crystals;" pp. 149-68 in *Proc. Conf. on Nuclear Applications of Nonfissionable Ceramics*. Edited by A. Boltax and J. H. Handwerk. American Nuclear Society, Hinsdale, Illinois, 1966.
24. M. H. Leipold, "Impurity Distribution in MgO," *J. Am. Ceram. Soc.*, 49 (9) 498-502 (1966).
25. R. B. Day and R. J. Stokes, "Mechanical Behavior of Magnesium Oxide at High Temperatures," *J. Am. Ceram. Soc.*, 47 (10) 493-503 (1964).
26. R. B. Day and R. J. Stokes, "Mechanical Behavior of Polycrystalline Magnesium Oxide at High Temperatures," *J. Am. Ceram. Soc.*, 49 (7) 345-54 (1966).
27. T. G. Langdon and J. A. Pask, "Effect of Microstructure on Deformation of Polycrystalline Magnesium Oxide," *J. Am. Ceram. Soc.*, (in press).
28. T. G. Langdon and J. A. Pask, "The Examination of Polycrystalline MgO by Transmission Electron Microscopy;" pp. 594-602 in *Ceramic Microstructures*. Edited by R. M. Fulrath and J. A. Pask. John Wiley and Sons, New York, 1968.

FIGURE CAPTIONS

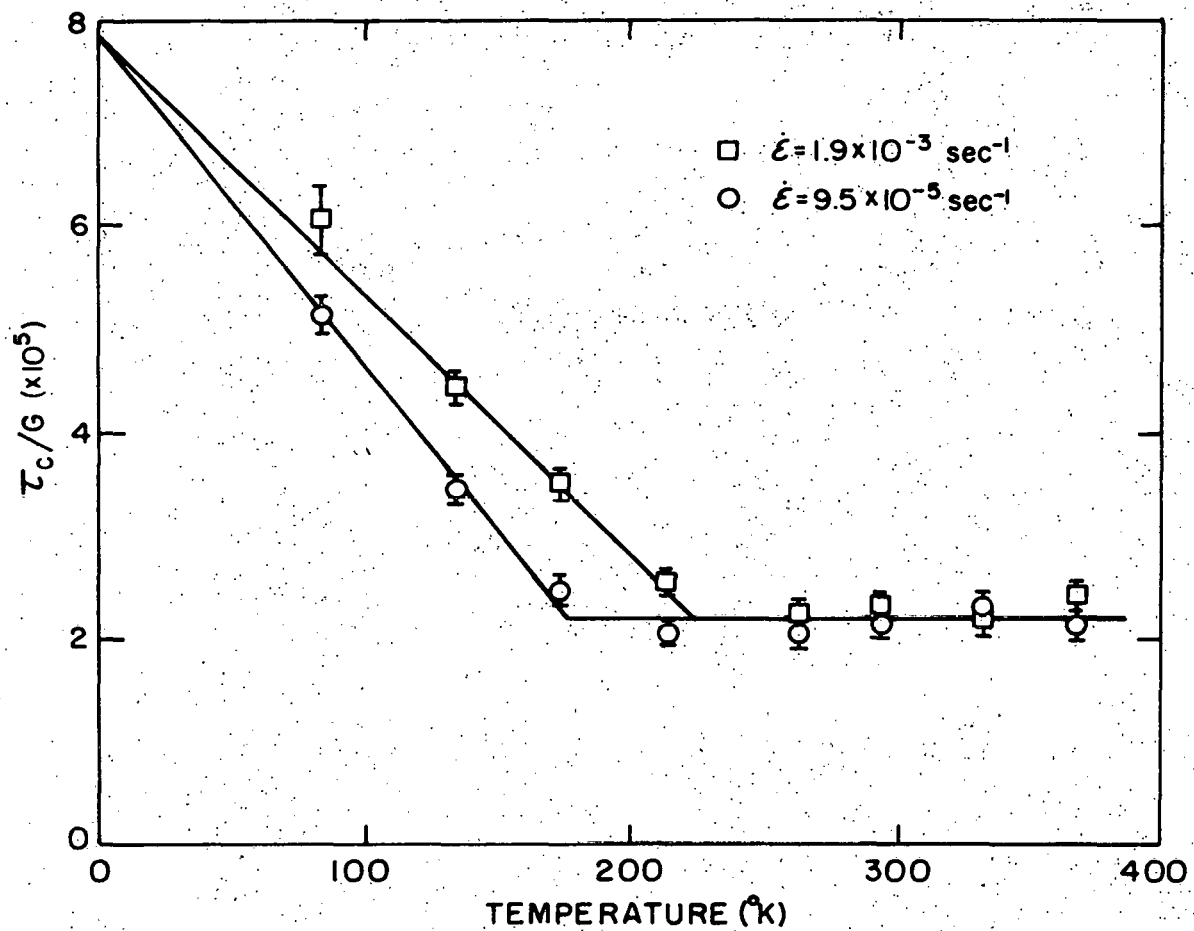
- Fig. 1. Schematic representation of the temperature dependence of the critical resolved shear stress (or the yield stress) up to the absolute melting temperature, T_m , for strain rates of $\dot{\epsilon}_1$, $\dot{\epsilon}_2$ and $\dot{\epsilon}_3$. Region I is thermally-activated, region II is athermal, region III is diffusion controlled, and region IV represents viscous damping.
- Fig. 2. Normalized critical resolved shear stress (τ_c/G) as a function of temperature for NaCl single crystals tested at two different strain rates.⁴
- Fig. 3. Flow stress as a function of temperature for MgO single crystals tested at strain rates differing by over seven orders of magnitude.⁵
- Fig. 4. Yield stress as a function of temperature for MgO single crystals having $\langle 100 \rangle$ and $\langle 111 \rangle$ loading axes.^{6,7,8} The $\langle 111 \rangle$ orientation yield stress at 560°C is 71,000 psi and at 360°C is 143,400 psi.
- Fig. 5. Stress-strain curves at 294°K for NaCl single crystals having Ca^{2+} concentrations of 2, 33 and 64 ppm, respectively.¹¹
- Fig. 6. Critical resolved shear stress as a function of temperature for "pure" and "impure" LiF single crystals showing effect of thermal history.¹²
- Fig. 7. Critical resolved shear stress for MgO single crystals tested at room temperature as a function of the molar concentration

- Fig. 8. Temperature variation of the effective stress for LiF single crystals containing 75 ppm of magnesium in solution (experimental data of Johnston¹²).¹⁸
- Fig. 9. Microstructures of four types of polycrystalline MgO: type 1 (lower left), 2 (lower right), 3 (upper left) and 4 (upper right).
- Fig. 10. Microstructure of type 5 polycrystalline MgO.
- Fig. 11. Stress-strain curves for six types of polycrystalline MgO at 800°C.
- Fig. 12. Stress-strain curves for six types of polycrystalline MgO at 1000°C.
- Fig. 13. Yield stress as a function of temperature for MgO single crystals with $\langle 100 \rangle$ and $\langle 111 \rangle$ loading axes, and for polycrystalline specimens of types 1-6. The closed symbol for type 1 at 1000°C is a fracture stress in the absence of yielding.
- Fig. 14. Stress-strain curves for MgO single crystals having a $\langle 111 \rangle$ loading axis.^{7,8}



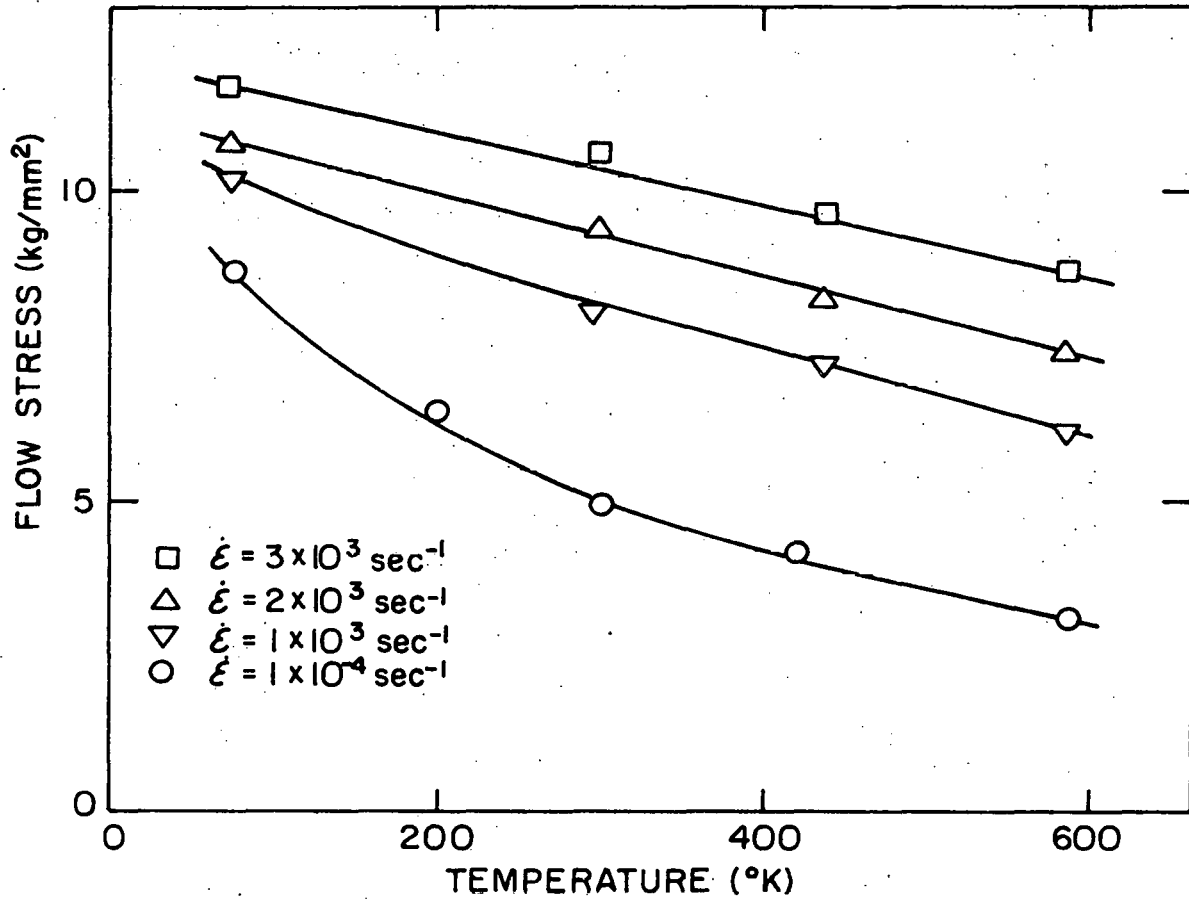
XBL 7011-7074

Fig. 1.



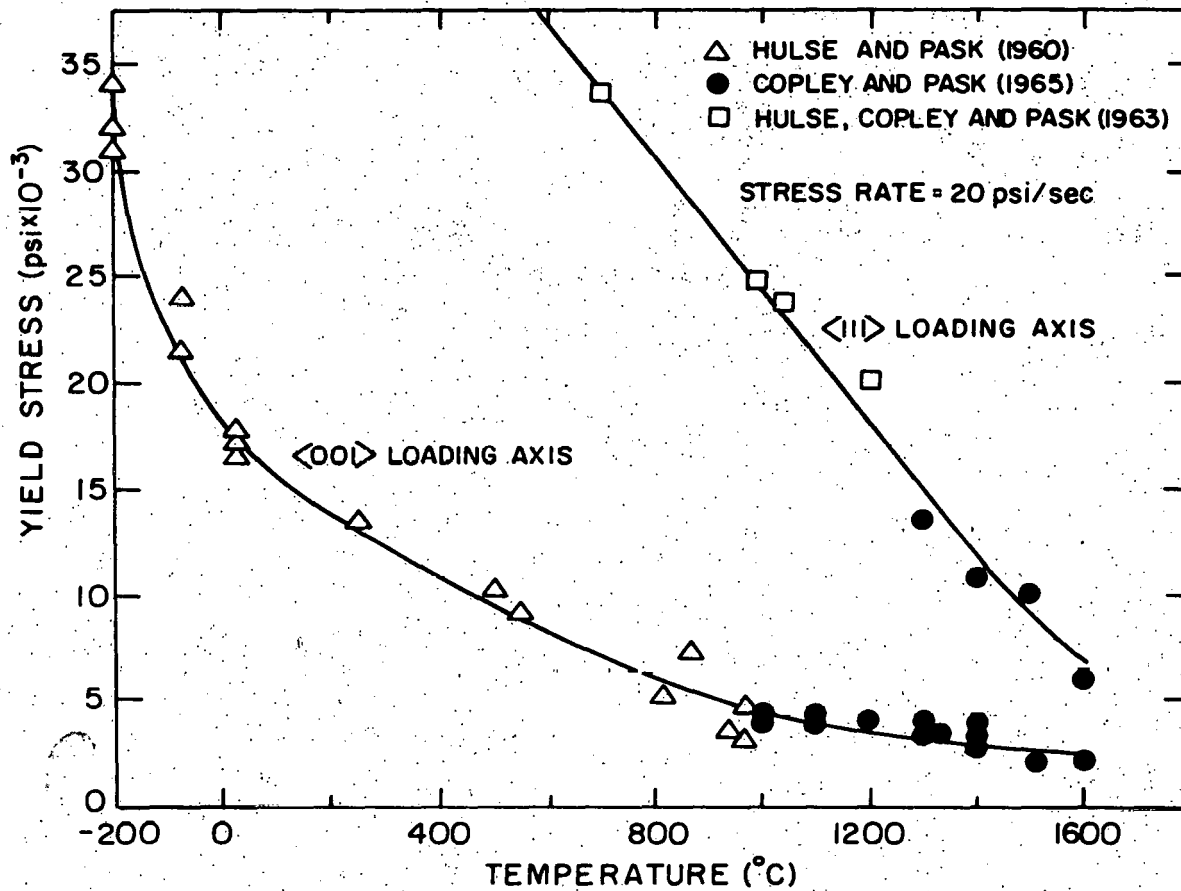
XBL 7011-7069

Fig. 2.



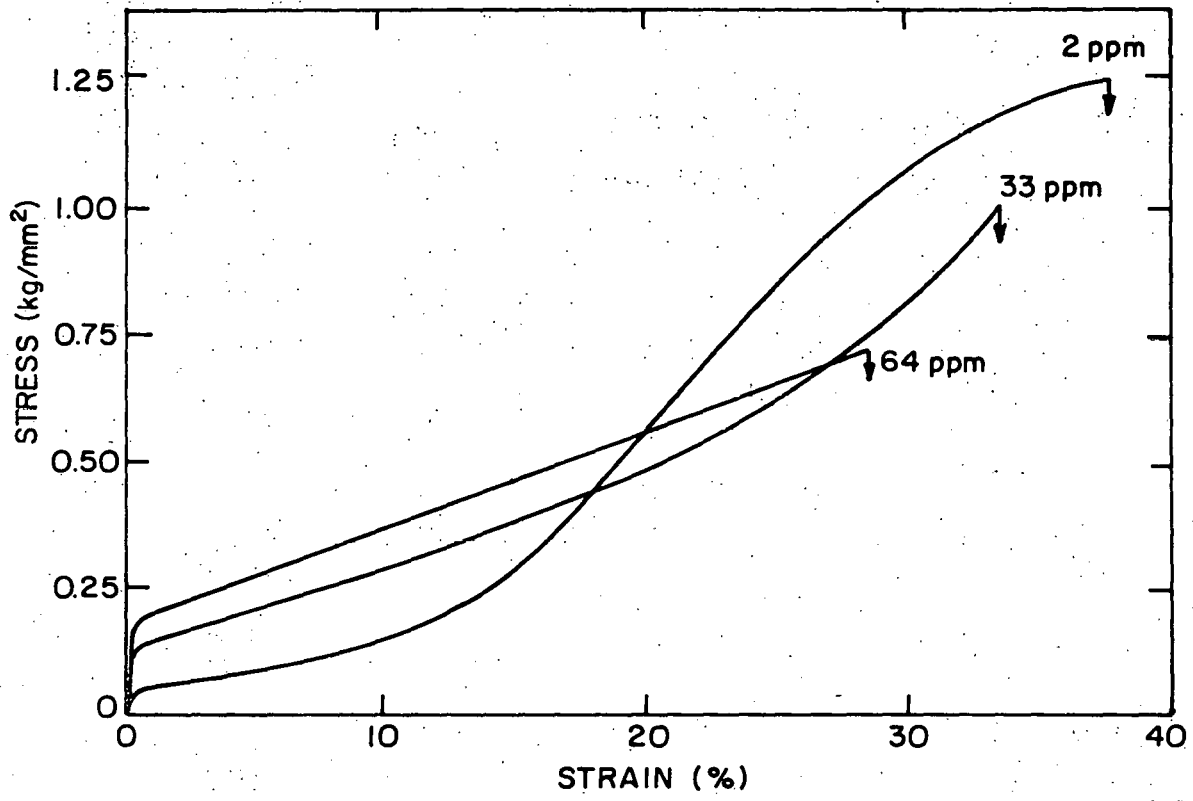
XBL 7011-7070

Fig. 3.



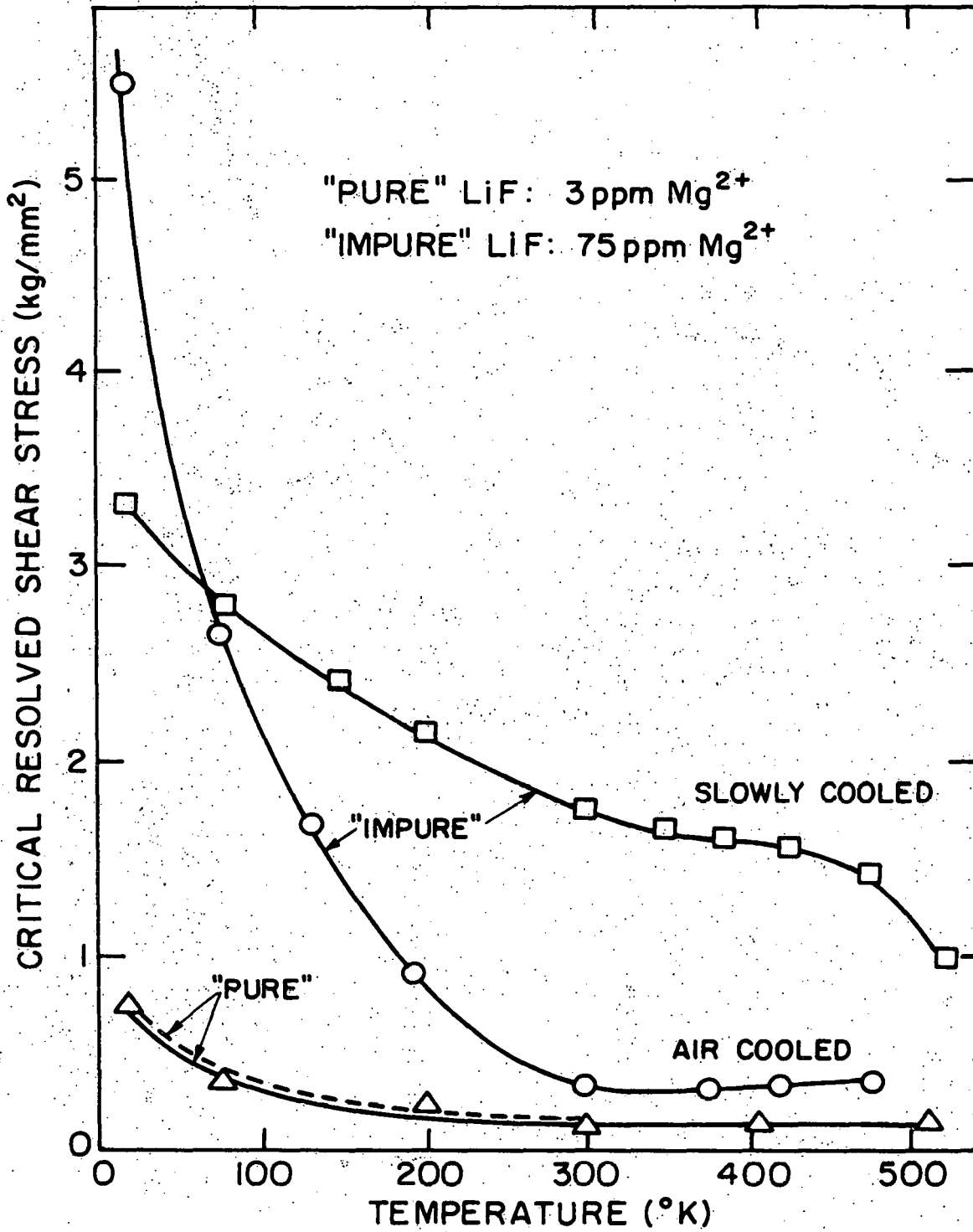
XBL 7011-7080

Fig. 4.



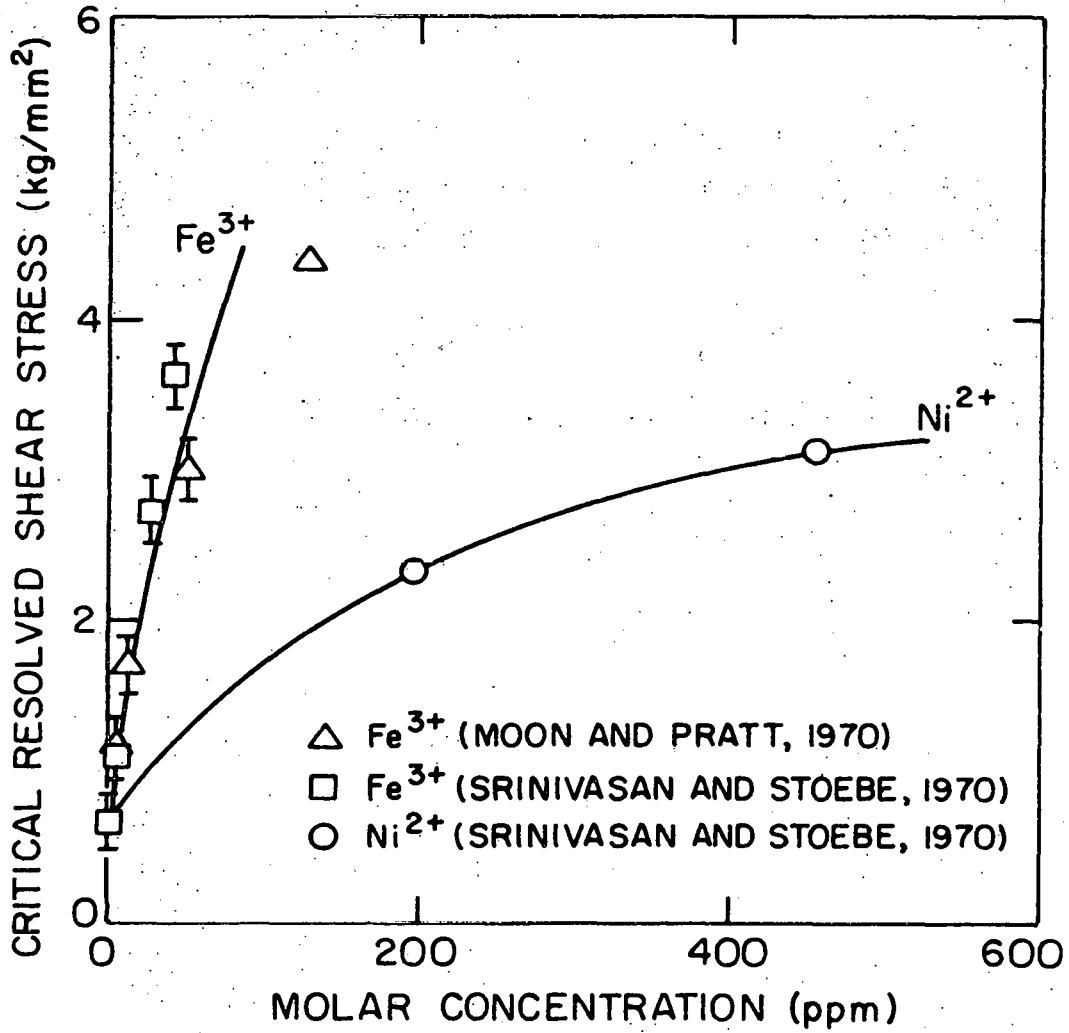
XBL 7011-7078

Fig. 5.



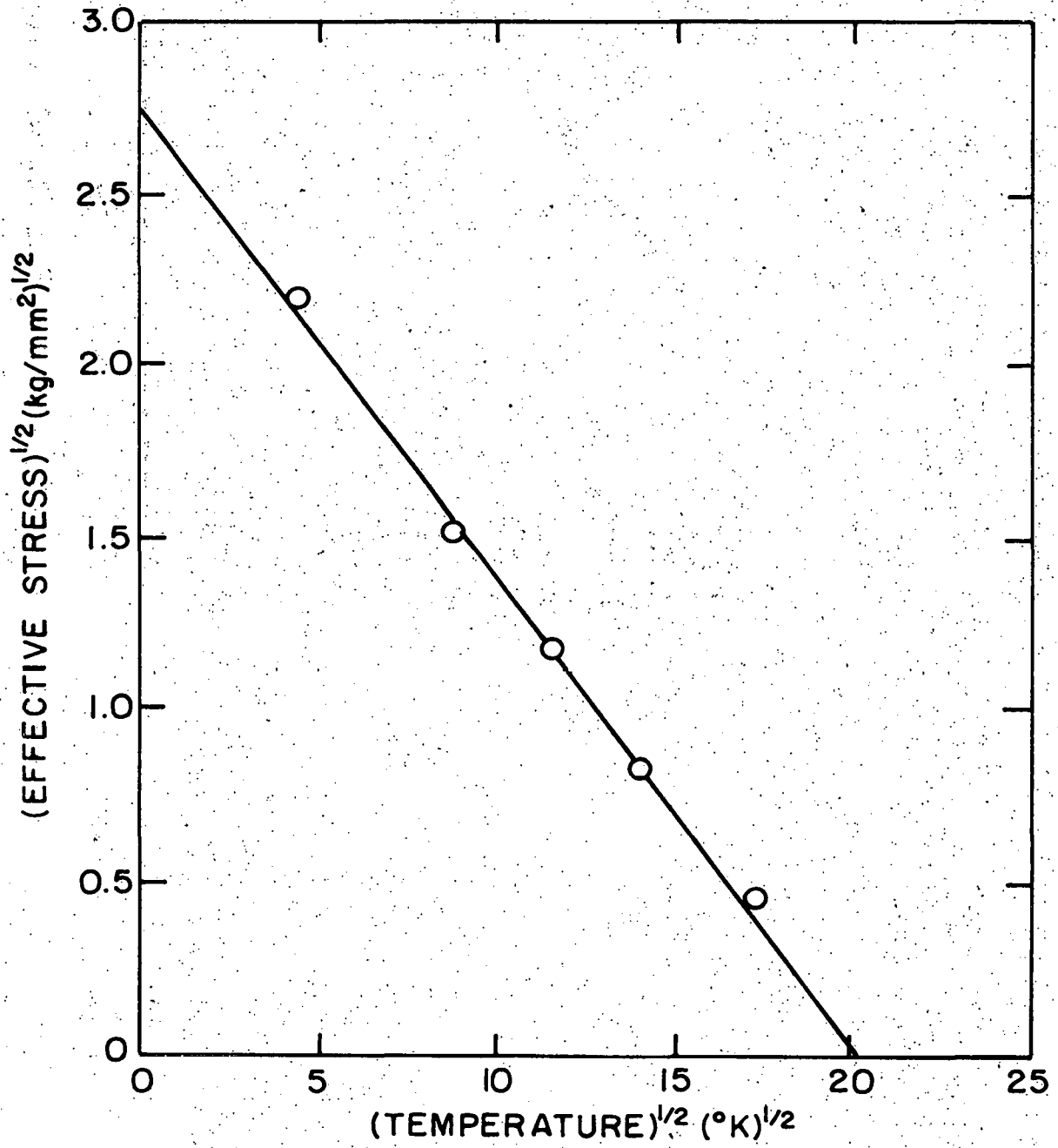
XBL 7011-7076

Fig. 6.



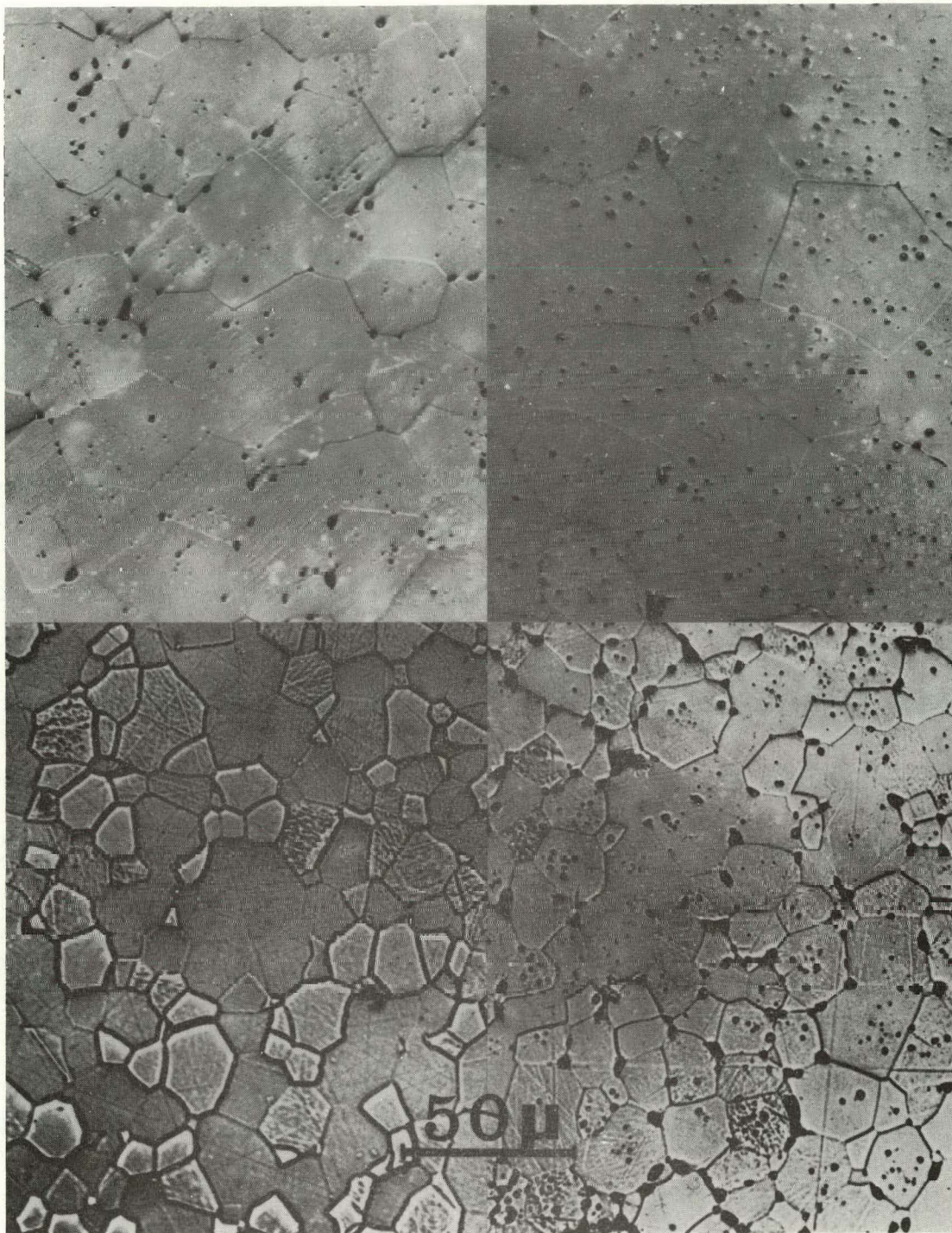
XBL 7011-7073

Fig. 7.



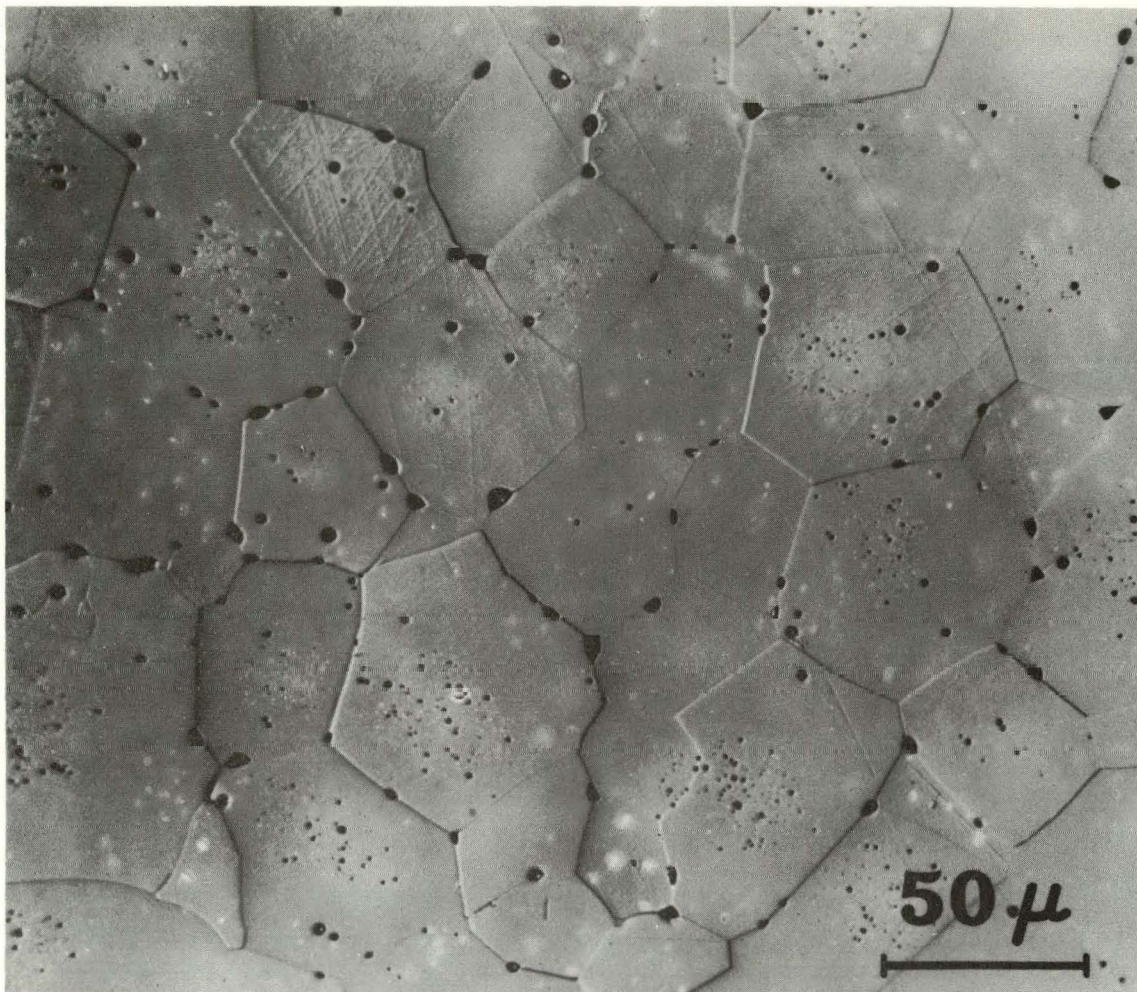
XBL 7011-7079

Fig. 8.



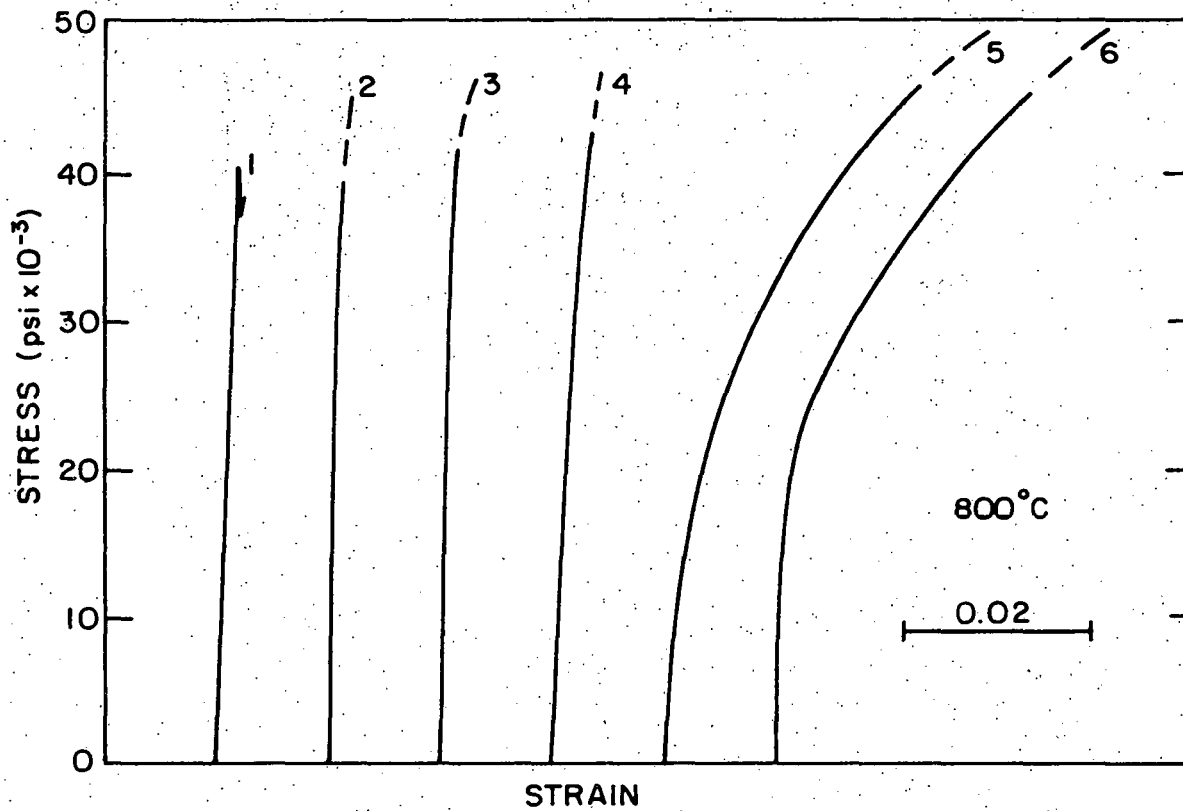
XBB 679-5600

Fig. 9.



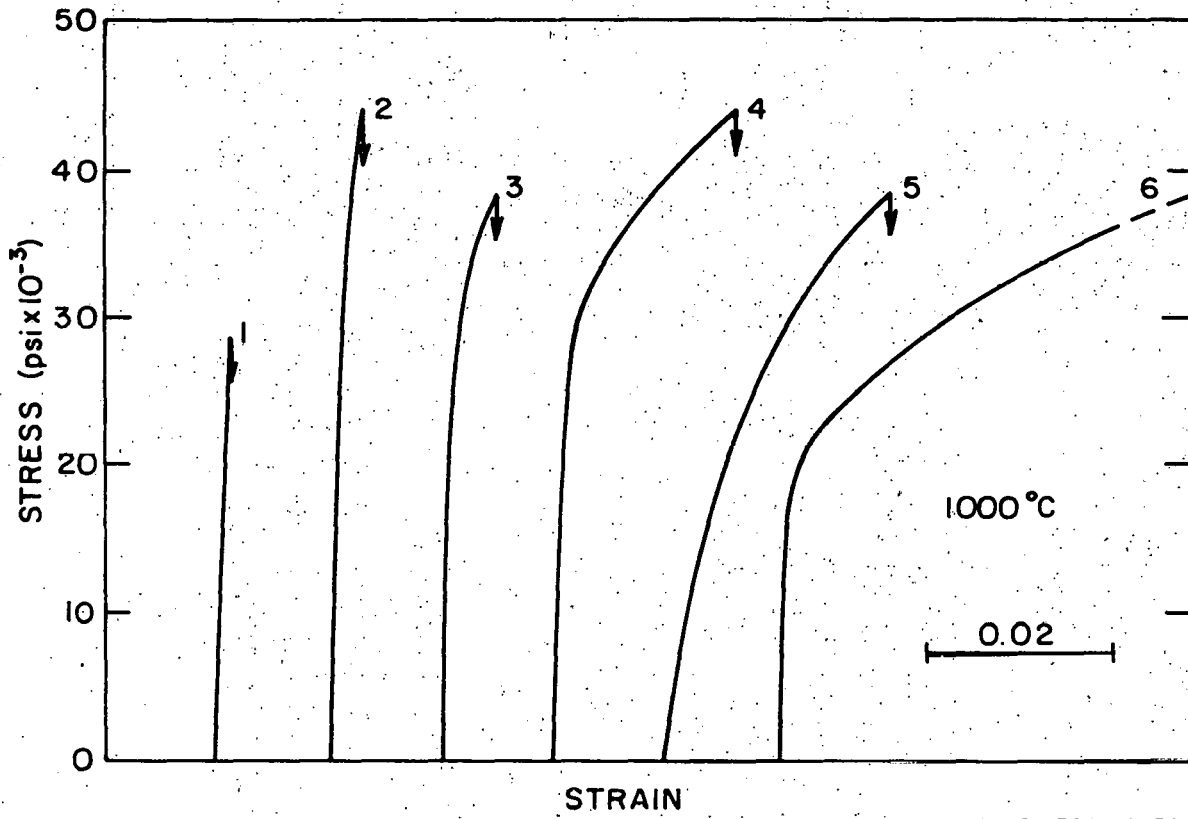
XBB 679-5519

Fig. 10.



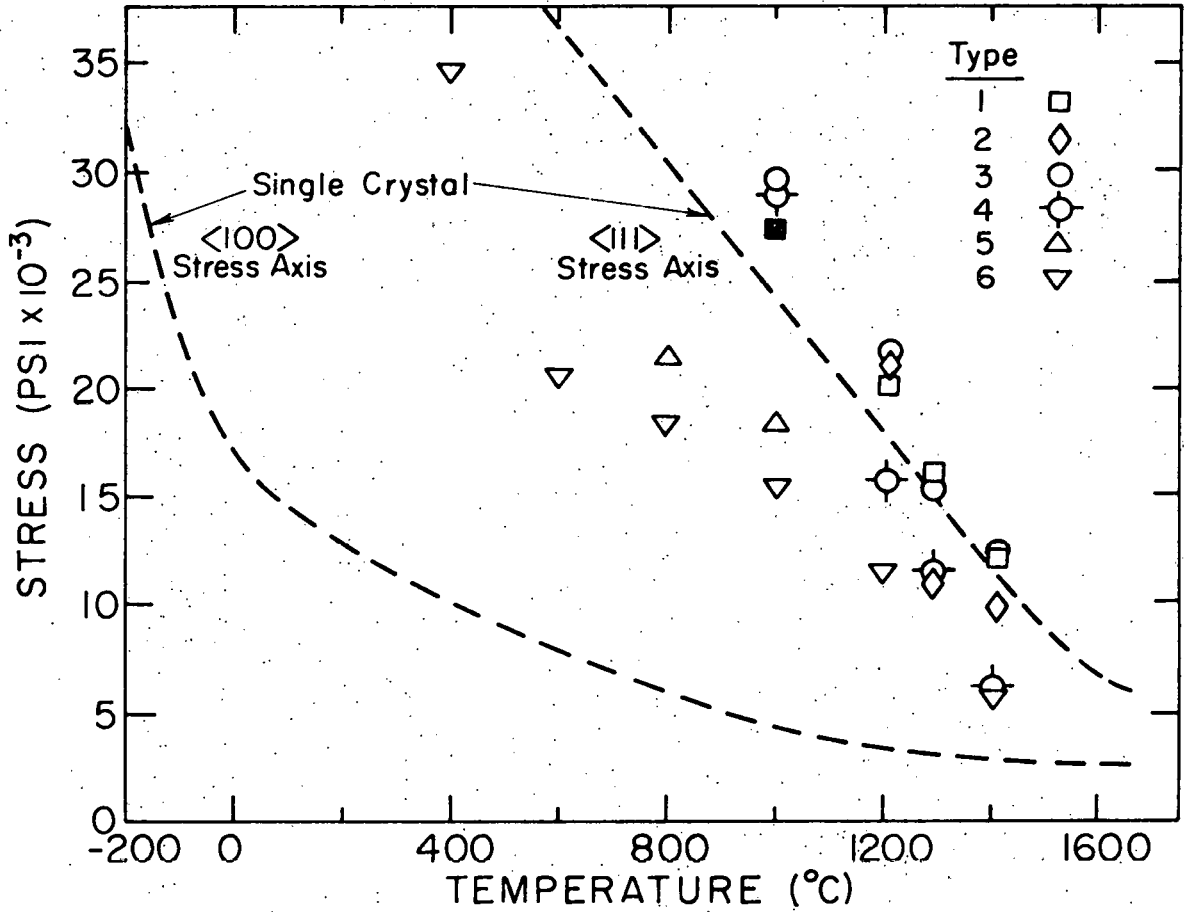
XBL 7011-7074

Fig. 11.



XBL 7011-7072

Fig. 12



XBL 7010-6721

Fig. 13.

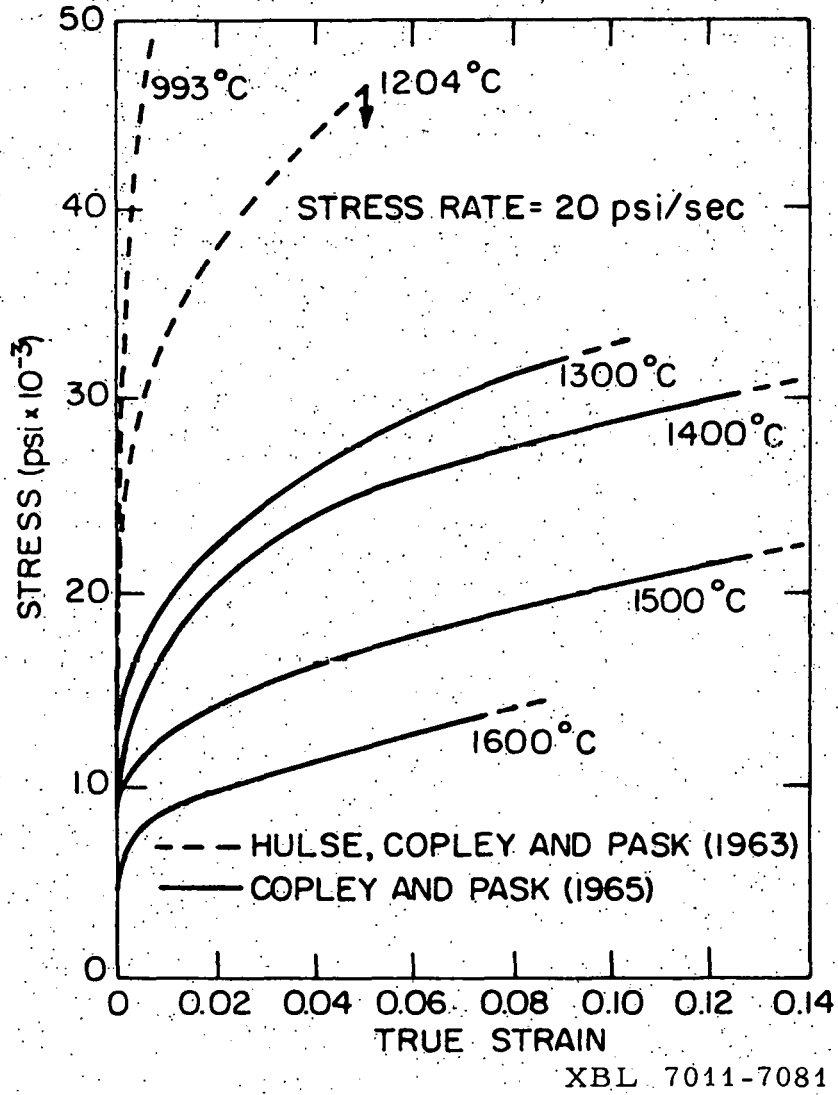


Fig. 14.

LEGAL NOTICE

This report was prepared as an account of Government sponsored work. Neither the United States, nor the Commission, nor any person acting on behalf of the Commission:

- A. Makes any warranty or representation, expressed or implied, with respect to the accuracy, completeness, or usefulness of the information contained in this report, or that the use of any information, apparatus, method, or process disclosed in this report may not infringe privately owned rights; or*
- B. Assumes any liabilities with respect to the use of, or for damages resulting from the use of any information, apparatus, method, or process disclosed in this report.*

As used in the above, "person acting on behalf of the Commission" includes any employee or contractor of the Commission, or employee of such contractor, to the extent that such employee or contractor of the Commission, or employee of such contractor prepares, disseminates, or provides access to, any information pursuant to his employment or contract with the Commission, or his employment with such contractor.

